

PRELIMINARY RESULTS OF THE U.S. POOL-BOILING COILS FROM THE IFSMTF FULL-ARRAY TESTS\*

J. W. Lue, L. Dresner, M. S. Lubell, J. N. Luton, T. J. McMannamy, and S. S. Shen  
Oak Ridge National Laboratory  
Oak Ridge, Tennessee 37831

Abstract

The Large Coil Task to develop superconducting magnets for fusion reactors, is now in the midst of full-array tests in the International Fusion Superconducting Magnet Test Facility at Oak Ridge National Laboratory. Included in the test array are two pool-boiling coils designed and fabricated by U.S. manufacturers, General Dynamics/Convair Division and General Electric/Union Carbide Corporation. So far, both coils have been energized to full design currents in the single-coil tests, and the General Dynamics coil has reached the design point in the first Standard-I full-array test. Both coils performed well in the charging experiments. Extensive heating tests and the heavy instrumentation of these coils have, however, revealed some generic limitations of large pool-boiling superconducting coils. Details of these results and their analyses are reported.

Introduction

The Large Coil Task (LCT) to develop superconducting magnets for fusion reactors, is now in the midst of full-array, six-coil tests in the International Fusion Superconducting Magnet Test Facility (IFSMTF) at Oak Ridge National Laboratory. Six D-shaped coils of 2.5- x 3.5-m bore are installed in the test facility in a compact toroidal array. Included in the array are two pool-boiling coils designed and fabricated by U.S. manufacturers, General Dynamics/Convair Division (GD) and General Electric/Union Carbide Corporation (GE).

The GD coil<sup>1</sup> is constructed of conductors with a compact monolithic structure consisting of a Rutherford-style NbTi superconducting cable soldered into the slot of a rectangular copper stabilizer. Side fins are machined along the stabilizer to provide extra surface area for cooling and to increase the local liquid helium inventory. The conductor is graded into 3 sizes and edge-wound into 14 layers. Interturn and interlayer insulation sheets direct helium bubbles in a way that minimizes accumulation at the top of the winding. This coil has previously been cooled down and electrically tested in the Partial-Array Test.<sup>2</sup> The GE coil<sup>3</sup> is constructed of conductors with semi-monolithic subelements cabled around a copper core. The conductor is graded into 3 sizes and flat-wound into 7 pancakes (with 12 active pies and 2 dummy pies) without interpancake cross-cooling channels.

Both GD and GE coils cooled down slowly and smoothly, together with all other coils and the test facility.<sup>4</sup> Electrical tests of all six coils were performed individually in a series of single-coil tests. In addition to charging up to 100% design currents, both the GD and GE coils were also subjected to simulated nuclear heating tests and stability measurements. In the ongoing full-array tests, the GD coil was the first one tested to the design point of 8-T field at full current. Selected results of these tests and their analyses are reported in this paper.

\*Research sponsored by the Office of Fusion Energy, U.S. Dept. of Energy, under Contract No. DE-AC05-84OR-21400 with Martin Marietta Energy Systems, Inc.

Simulated Nuclear Heating Tests

All fusion reactors will produce significant nuclear heating. The actual amount impinging on the superconducting magnets is strongly dependent on machine design. For any particular fusion concept, the level can be attenuated by the amount of shielding used between the fusion core and superconducting magnet system. However, the more shielding used, the larger the machine becomes and, therefore, the cost is greater. One is, therefore, loath to increase the shielding any more than the absolute minimum given by the maximum nuclear heating that the superconducting coils can withstand. Since this amount is unknown for superconducting magnets, the recent design studies for the Tokamak Fusion Core Experiment (TFEX)<sup>5</sup> assumed nuclear heating rates of 10 MW/cm<sup>2</sup> for the nominal design and 50 MW/cm<sup>2</sup> for a high-performance (optimistic) design. The experiments described in this paper are the first to explore this important problem in superconducting magnets of any appreciable size. Never before have large superconducting magnets been constructed with heaters embedded in their windings.

To simulate the nuclear heating and to measure the stability of the coils, strip heaters are built into both pool-boiling coils, each covering half a turn (4 to 6 m long) of the winding. The GD coil heaters are made of nichrome wires, insulated with Kapton, embedded on the top of the superconducting cable and covered with solder. The GE coil heaters are made of Inconel tape, insulated with Kapton, and bonded to the surface of the subelement with epoxy. Figure 1 shows the location of the heaters in each coil.

After the coil was energized to some current level and held steady, a simulated nuclear heating test was

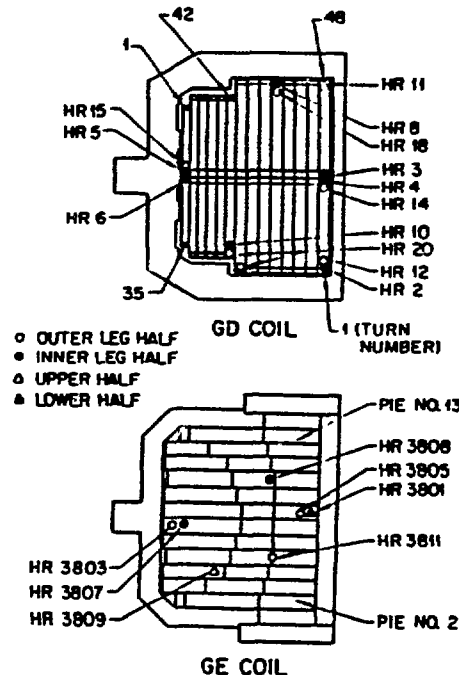


Figure 1. Locations of strip heaters in the GD and GE coils.

**MASTER**

DISTRIBUTION OF THIS DOCUMENT IS UNLIMITED

*Jsw*

performed by powering all the heaters in parallel for 60 s. The heating time was chosen to obtain a steady-state environment without creating too much pressure rise in the coil and undue heat load on the refrigerator. On the GD coil up to 825 W of total heating power was applied to the 13 heaters, which corresponds to local unit conductor heating of 44 to 66 mW/cm<sup>2</sup> (because of conductor grading and different heater lengths). The test was performed up to 100% design current (10.2 kA) in the single-coil test. All runs were uneventful in that no normal zone nor quenching was observed.

On the GE coil, a total heating of 845 W on six heaters, which corresponds to local unit conductor heating of 86 to 140 mW/cm<sup>2</sup>, was successfully applied to the coil up to 80% design current. But, when the heating power was almost doubled to 1510 W (150 to 250 mW/cm<sup>2</sup>), a normal zone was observed shortly after heating began. Although heating was stopped in 15 s, the normal zone propagated and the coil quenched. Figure 2 shows that the conductor voltage over pie 3-4 (X-data), which contains heater HR3809 on the first turn of 4-T grade conductor, started the normal zone propagation. The applied heating power was considerably higher than the design value, yet quenching was still unexpected. Copious vapor accumulation on the upper half of the pancake, which has no cross-flow channels, can explain this result.

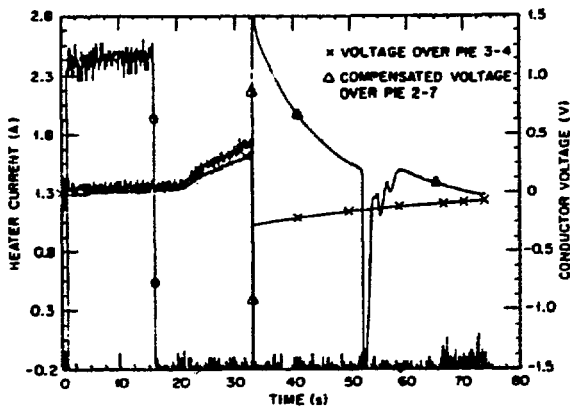


Figure 2. Normal zone propagation and coil quenching of GE coil during a simulated nuclear heating test. Note that after the dump at 33 s, the voltage signals were attenuated.

### Stability Measurements

The purpose of the stability measurements was twofold: (1) to verify attainment of the stability aimed for in the design and (2) to demonstrate scalability (i.e., to demonstrate that the design of full-scale magnets could be based on short-sample heat transfer experiments). The stability of the GD coil was measured in both single-coil and Standard-I full-array tests, while the stability of the GE coil has been measured so far only in the single-coil tests. In all tests two half-turn heaters positioned in one turn were pulsed in parallel to drive the conductor normal. The conductor temperature and voltage in the heated zone were recorded to monitor the recovery process.

### GD in Single-Coil Test

In the single-coil test unconditional recovery was observed in the GD coil up to 100% design current. Figure 3 shows the normalization and recovery of the inner leg of a heated turn at  $I^* = 100\%$  ( $I^* = I/I_{design}$ ). When recovery of a pool-cooled

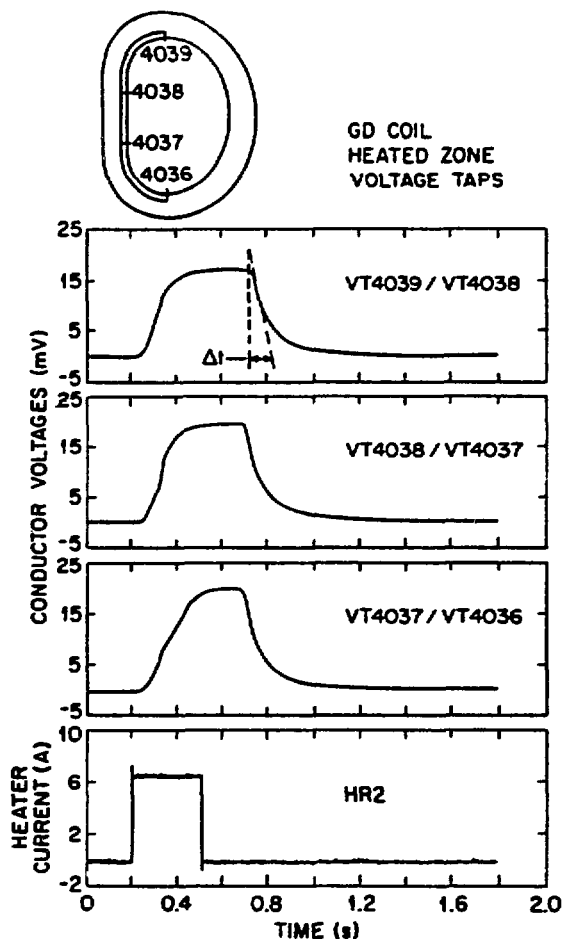


Figure 3. Recovery of normal zones from a heater pulse on heaters HR2 and HR12 in GD coil at  $I^* = 100\%$  in single-coil test.

magnet is unconditional (rather than cold-end), the heat flux during recovery can be obtained from the curve of normal-zone voltage versus time in the following way. The recovery process can be described by the space-independent heat balance equation

$$A S \frac{dT}{dt} = -q(T)P + I V_G(T), \quad (1a)$$

where  $G(T)$  is the current-sharing function

$$G(T) = \begin{cases} 0, & T < T_{cs} \\ (T - T_{cs}) / (T_c - T_{cs}), & T_{cs} < T < T_c \\ 1, & T_c < T \end{cases} \quad (1b)$$

and  $A$  is the cross-sectional area of the conductor,  $S$  is its heat capacity per unit volume,  $T$  is its temperature,  $t$  is the time,  $q$  is the heat flux,  $P$  is the cooled perimeter,  $I$  is the transport current,  $V_G$  is the saturation voltage per unit length of conductor,  $T_{cs}$  is the current-sharing threshold temperature, and  $T_c$  is the critical temperature. When  $T = T_c$ , a sharp knee occurs in the voltage-time curve as the recovering superconductor reenters the current-sharing range. At that temperature Eq 1 becomes

$$AS(T_c) \left( \frac{dT}{dt} \right)_{T=T_c} = -q(T_c)P + IV \quad (2)$$

All of the terms in Eq 2 are known from the present experiments except  $q$ , so we can determine  $q$  from the experimental data.

In the current-sharing range, the normal-zone voltage is a linear function of  $T$ , having its maximum (saturated) value  $V_m$  at  $T = T_c$  and the value zero at  $T = T_{cs}$ . Then

$$\left( \frac{dT}{dt} \right)_{T=T_c} = - \frac{T_c - T_{cs}}{\Delta t} \quad (3)$$

where  $\Delta t$  is the time at which the tangent to the voltage time curve crosses the line  $V = 0$  (see Fig. 3). From Eqs 2 and 3, the heat flux  $q(T_c)$  at full current is calculated to be  $0.11 \text{ W/cm}^2$ . This value of a vertical orientation of the conductor (straight leg) should be directly comparable with the fluxes reported by Christensen and Peck.<sup>6</sup> Their value for the same temperature rise is about  $0.23 \text{ W/cm}^2$ , or roughly twice as great as the value obtained from Eq 2. The most likely cause of this discrepancy is degradation of heat transfer due to copious production of vapor by the normalizing pulse.

#### GE in Single-Coil Test

The recovery of the GE coil, on the other hand, was unconditional at some locations and cold-end at others, notably at the top of the coil where the conductor became horizontal. Figure 4 shows the normalization and recovery of the upper half of a heated turn at  $I^* = 100\%$ . The top voltage trace (the outer third of the upper half) consists of five distinct regions: AB, in which the voltage rises as the zone is warmed by the heater above the current-sharing threshold  $T_{cs}$ ; BC, in which the voltage saturates, indicating that the temperature is greater than  $T_c$  everywhere; CD, in which part of the heated zone recovers unconditionally; DE, in which the remainder of the heated zone undergoes cold-end recovery; and EF, in which cold-end recovery continues but with a more rapid decline of voltage.

The flux from the unconditionally recovering part of the conductor into the helium can be calculated as explained above using Eq 2. However, since only a fraction of the heated zone recovers unconditionally, the right-hand side of Eq 3 must now be multiplied by  $1/f$  ( $= 2$  in this case). We find, then, that  $q(T_c) = 0.092 \text{ W/cm}^2$ . This flux can be compared with the fluxes directly measured by Walstrom for a small section of the same winding pack. For orientations between  $45$  and  $90^\circ$  to the horizontal, Walstrom's data give a flux  $q(T_c)$  of  $0.25 \text{ W/cm}^2$ , about 2.8 times the recovery heat flux obtained from the stability tests. Again the explanation of the discrepancy is copious vapor production by the heater.

The middle voltage trace which spans the uppermost third of the upper half-turn remains saturated until the moments when the voltage in each of its neighboring zones disappears (which, coincidentally, happen at the same time). Thus cold ends enter this heated zone from both sides simultaneously and propagate inwards. Cold-end recovery at full current but at a field of only  $5.5 \text{ T}$  also suggests that vapor accumulation is affecting heat transfer. The saturated Joule heat flux is only  $0.080 \text{ W/cm}^2$ , less than Walstrom's measured

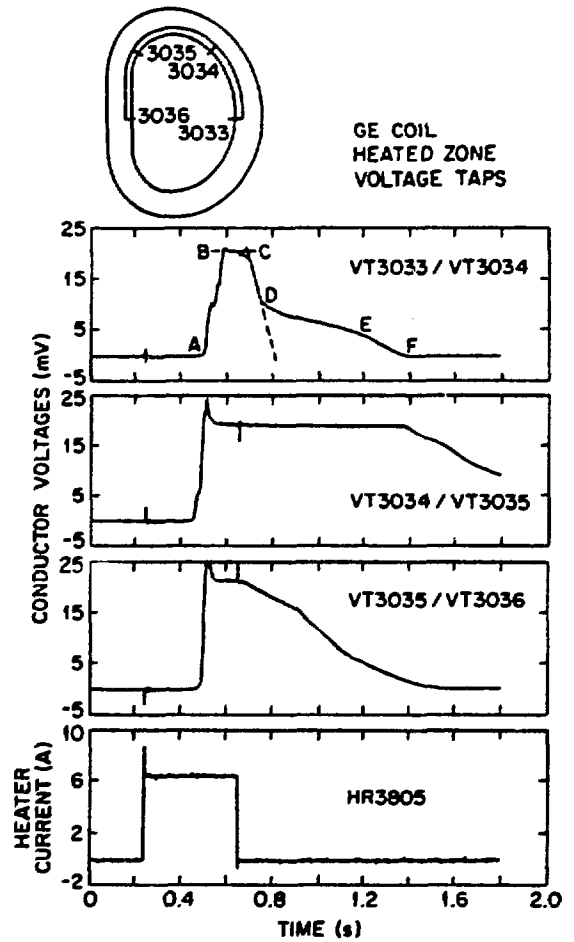


Figure 4. Recovery of normal zones from a heater pulse on heaters HR3805 and HR3801 in GE coil at  $I^* = 100\%$  in single-coil test.

value for a horizontal conductor and substantially less than his measured value for inclinations of as little as  $10^\circ$  to the horizontal.

It should be noted that because of the construction of the heaters described earlier, much higher energy pulses than were needed to normalize the conductor were used in these tests. In the GD test shown in Fig. 3, a 300-ms heat pulse of about  $360 \text{ mJ/cm}^2$  of unit conductor energy density was used. In the GE test shown in Fig. 4, a 400-ms pulse of  $480 \text{ mJ/cm}^2$  was used. These are far more serious tests than called for in the specifications, which require the coils to be able to recover from a half-turn normal without heat transfer degradation by a large initial vapor inventory.

#### GD in Full-Array Test

Cold-end rather than unconditional recovery was also observed in the GD coil when the stability measurement was made in the Standard-I full-array test. Figure 5 shows the result at  $100\%$  design current on GD and  $77\%$  current on all other background coils, which produced  $8.0 \text{ T}$  on the midplane of the GD coil (as compared with  $5.5 \text{ T}$  in the single-coil test). The middle-third zone did not start to recover until the top third recovered and the cold end reached it. It is also interesting to note that although the bottom third started to recover at the same time as the middle third, it did not recover any sooner than the middle third.

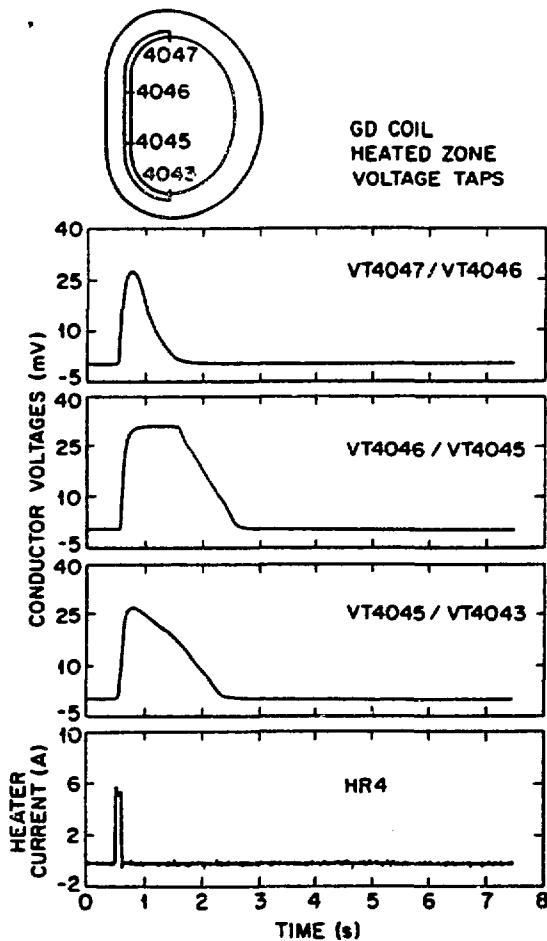


Figure 5. Recovery of normal zones from a heater pulse on heaters HR4 and HR14 in GD coil at the design point in full-array test.

The precaution to prevent vapor accumulation in the top of the winding may have caused partial vapor locking near the bottom of the coil at the inner ring. The heating pulse energy density in this test was reduced to 98 mJ/cm<sup>2</sup> to barely create a flat top for the normal zone. Similar cold-end recovery behavior was also observed when the test was done on the first turn of the 6-T grade conductor, which was predicted to be less stable than the 8-T grade conductor.

#### Standard-I Design-Point Tests

The Standard-I test of the full array was to achieve the design point of 8.0 T at the midplane of the test coil at 100% current and 80% current for the background coils. The GD coil was the first test coil. Because of different ampere-turns in the actually built coils, it was later calculated that 77% current in each of the background coils would be sufficient to produce 8.0 T at the GD-coil midplane. On the day of the first charge to design point, moisture in the bus lines of the EU coil was found to have caused severe degradation in the breakdown voltages. It was then decided to limit that coil's current to 60% and increase the other background coils' currents to compensate for the difference. The result of the first charge up to design point in the IFSMIF is shown in Fig. 6.

With the GD coil current at 99.4% and background currents at 60.1-86.6%, the field at the midplane of the GD coil reached 8.08 T. The maximum field at the

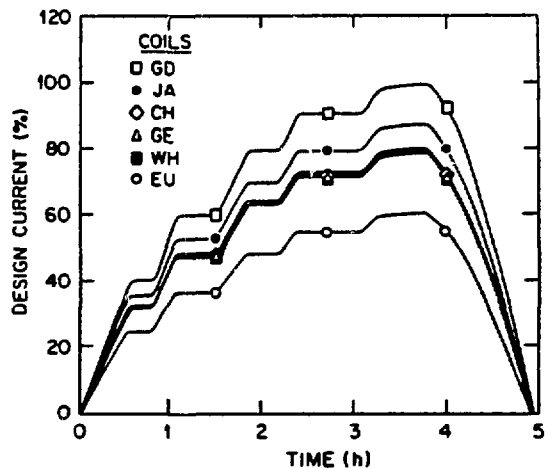


Figure 6. Current charges in the six coils during the first achievement of design point of the full array in IFSMIF.

corners of the straight leg was then between 8.2 and 8.3 T. This is the largest magnet ever built to reach 8 T. The total stored magnetic energy of the full-array was 570 MJ. The centering force on the GD coil was 39 MN. The largest out-of-plane load was placed on the neighboring Japanese (JA) coil with 6.4 MN pulling toward the GD coil. The subsequent stability tests on the GD coil were run with equal background coil currents of 77%, which reduced the out-of-plane load on the JA coil by about 10%.

#### Mechanical Behavior

Mechanical integrity of a superconducting coil the size of LCT coils is a great concern in the design and testing of these magnets. The implication of the test results in scaling to future, larger coils is also of great interest. Scores of strain gauges are attached on the winding and case of both the GD and GE coils to measure the hoop strain and compressive or tensile strain in the radial and axial directions, respectively. The mechanical behavior of both the GD and GE coils was also monitored by displacement transducers and acoustic emission (AE) sensors.

#### Strain Measurements

Figure 7 shows two of the high hoop strains on the winding of the GD coil in both single-coil and full-array tests. All data show roughly linear dependence on current squared (i.e., force), as expected. The differences in the strain readings between the single-coil and full-array tests are quite large, being 40% higher at the midplane of the outer leg (SE4315) and 2.3 times higher at the midplane of the inner leg (SE4302). These differences cannot be explained by the field increases at these points alone. Furthermore, the measured values are much higher than the predicted values. For the full-array results, SE4302 read 80% higher and SE4315 read 2.4 times higher than expected. The high reading of SE4315 at 1680  $\mu\epsilon$  was approaching the yield strain of the copper stabilizer.

Also shown in Fig. 7 are strain data on the coil case at the midplane of the outer leg. The measured values are very low compared with those on the conductors and are much lower than predicted; the value of 110  $\mu\epsilon$  at full-array test is about 2.5 times lower than that predicted.

Single-coil tests on the GE coil showed similar strain behavior to the GD coil. The predicted values

symmetrical as in the single-coil test and of the same magnitude.

#### Acoustic Emissions

Acoustic emissions were monitored by sensors attached to the coil cases.<sup>4</sup> The signals were recorded by an FM recorder. Real-time signals of selected channels were watched on a scope, together with compensated voltage of the test coil. Observation of the real-time signals indicated that both coils show qualitatively similar behaviors. Very few AEs were seen below about 60% design currents. On the virgin run, the frequency and size of AE events increased steadily toward higher currents. However, there was no clear correspondence between AE and compensated coil voltage. The latter increased monotonically toward design current. In the rampdown and in subsequent runs, the AEs were much smaller and less frequent.

All three means of monitoring the mechanical behavior of the coils seem to point out the fact that the mechanical coupling between the winding and the case is rather poor. The winding is moving and taking almost all the charging loads and does not transfer them to the case.

#### Other Results and Summary

The low-voltage breakdown withstand capability of the GD coil, as was reported before,<sup>2</sup> has deteriorated further during the present test period. At the beginning of the single-coil test, the breakdown voltage was measured to be about 460 V. A dump resistor of 52 mΩ was used to extract the energy out of the coil from a coil dump. The measured decay time constant was 36 s. Typically 97% of the initial magnetic energy stored in the coil was dissipated in the dump resistor. By the time of the Standard-I test, the breakdown voltage was down to about 260 V. It was decided then to lower the dump resistor to 26 mΩ so that in the event of a dump from full current, the terminal-to-ground voltage would be limited to about half the measured breakdown voltage. However, because of the mutual inductances from the background coils, the decay time constant more than doubled to 84 s. This is more than twice as long as any of the other coils. Thus in the case of a dump, much of the initial mutual energy will be transferred to the GD coil, and therefore a high conductor temperature and considerable heating of the dump resistor can be expected during a dump from high currents.

Table 1 summarizes the test results obtained so far, together with some relevant parameters of the GD and GE coils.

#### Conclusion

In general, we are pleased with the performances of the two U.S. pool-boiling coils. In particular, despite all the difficulties experienced during the manufacturing process of the GE coil, it succeeded in its first cooldown and in all electrical testing. It was charged to its 100% design current without tripping or quenching, as was done on all other coils in the IFSMT.

The achievement of the 8-T design point on the GD coil at 100% design current with background coils at currents ranging from 60.1-86.8% is very gratifying. It was accomplished with shortcomings of various natures, such as low breakdown voltage in the GD coil and some bus lines, different ampere-turns in the coils, under-capacity refrigerator system, and six unseasoned power supplies.

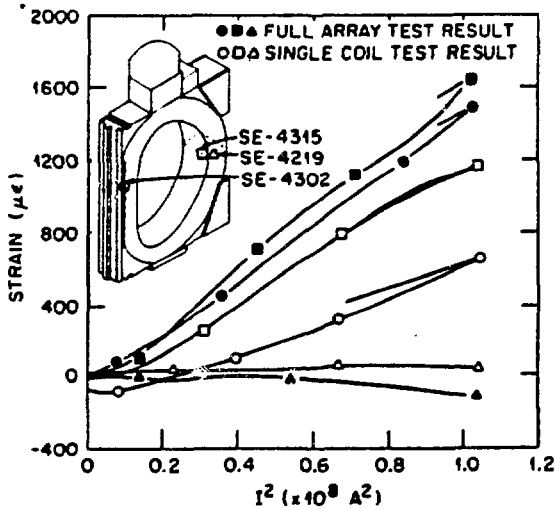


Figure 7. Strain readings on coil winding (SE4302 and SE4315) and coil case (SE4219) of GD coil in single-coil and full-array tests.

on the winding at the midplane of both the inner leg and outer leg registered almost exactly the same strain reading at 100% design current. The strains on the case are also low, none read higher than 200 µε.

#### Winding Displacement

The Magnetic Slug Displacement Transducer (MSDT) measured the winding displacement from the coil case. Figure 8 shows the results in single-coil tests of GD and GE coils to 100% design current. In the axial direction, both coils showed about the same displacement from the side plates, about 0.79 mm (31 mil) each in the single-coil tests to 100% design currents. However, the displacements away from the inner ring of the coil case were about twice as large on the GE coil (3.2 mm) as on the GD coil (1.5 mm), and the values were roughly the same at either the midplane of the inner leg or the outer leg. Because of the conductor configuration and interturn insulation, it was expected that the GE coil has a rather spongy winding. It was surprising to find that the GD coil also had a spongy winding. During the full-array test the out-of-plane load received by the GD coil was about two orders of magnitude lower than the in-plane load. The displacements from the side plates were as

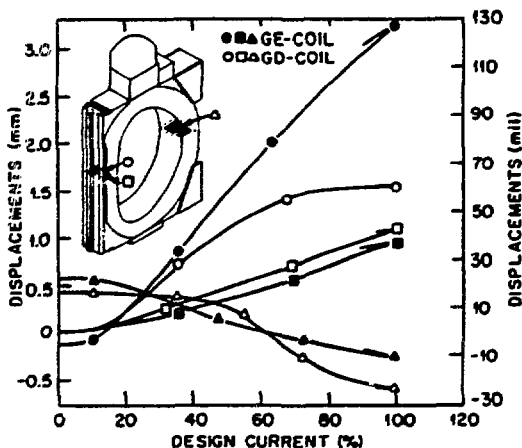


Figure 8. Comparison of winding displacements in GD and GE coils in single-coil tests.

Table 1. Summary of Coil Test Results

Item	GD coil	GE coil
Design current (A)	10,200	10,500
Ampere-turns (MA)	6.41	6.53
Residual resistance ratio	187	121
Self-inductance (H)	1.84	1.81
Dump resistor (mΩ)	52/26 <sup>a</sup>	59
Discharge time constant (s)	36/84 <sup>a</sup>	31/40 <sup>a</sup>
Measured breakdown voltage before coil testing (V)	460/260 <sup>a</sup>	>1200 <sup>b</sup>
Fraction of energy removed by dump resistor	97/96 <sup>a</sup>	96/87 <sup>a</sup>
Maximum field achieved at midplane (T)	8.1	6.9 <sup>a</sup>
Stability measurement results	Unconditional recovery to I* = 100% cold-end recovery at I* = 100% <sup>a</sup>	Cold-end recovery at I* ≥ 80%
Maximum simulated nuclear heating energy density tested without a quench (mW/cm <sup>3</sup> )	66	140 <sup>c</sup>
Maximum strains on conductor (με)	1200/1680 <sup>a</sup>	1200
Maximum strains on coil case (με)	210/190 <sup>a</sup>	180
Maximum strains on support collar (με)	1200/180 <sup>a</sup>	1150
Centring force in GD Standard-I test (MN)	39	31
Out-of-plane load in GD Standard-I test (MN)	2.5	1.6
Displacement of winding from case inner ring (mm)	1.5	3.2
Displacement of winding from side plates (mm)	0.79/0.79 <sup>a</sup>	0.79/0.79 <sup>a</sup>

<sup>a</sup>Standard-I full-array test value with GD as the test coil.

<sup>b</sup>Passed tests to 1200 V without a breakdown.

<sup>c</sup>At I\* = 80%.

The heavy instrumentation in the GD and GE coils, though presenting tremendous difficulties in the assembly of the coils, has generated some very informative results. Two notable generic limitations of large pool-boiling superconducting coils have been revealed: (a) Vapor accumulation and vapor locking can severely degrade the heat transfer of the conductor. The normal zone propagation in the simulated nuclear heating test of the GE coil and the cold-end rather than unconditional recovery observed in both coils in the stability test can all be explained by these effects. (b) The mechanical coupling between the winding and case of a pool-boiling coil is poor. This is manifested by the facts that the measured strains on the conductor are much higher than those on the case and the former are higher while the latter are lower than predicted; the displacement of the winding from the case is substantial under loads; the correlation of AE signals that were monitored on the coil case to the compensated voltage spikes that were most likely due to conductor motions is poor for the pool-boiling coils.

### Acknowledgments

The dedicated and skillful operators of the test facility, working around the clock under the supervision of W. A. Fietz, are gratefully appreciated. The ever-patient engineering and computing help of C. T. Wilson, R. E. Wintenberg, L. R. Bayor, R. J. Wood, and D. T. Fehling is invaluable. The interest and help of onsite foreign participants are also appreciated.

### References

1. D. S. Hackley et al., Proc. 8th Symp. on Engineering Problems of Fusion Research, Vol. 3, 1163, IEEE, New York, 1979.
2. J. W. Lue et al., Fusion Technol., Vol. 8(1), Pt. 2A, 807, 1985.
3. R. Quay et al., Proc. 8th Symp. on Engineering Problems of Fusion Research, Vol. 3, 1154, IEEE, New York, 1979.
4. P. N. Haubenreich et al., "Experience with the cooldown of superconducting magnet coils in the LCT," paper presented at the 14th Symp. on Fusion Technology, Avignon, France, September 8-12, 1986.
5. "TFCX Pre-conceptual Design Review," Princeton Plasma Physics Laboratory, June 6-8, 1984.
6. E. H. Christensen and S. D. Peck, Adv. Cryog. Eng., 27, 327, 1982.
7. P. L. Walstrom, Adv. Cryog. Eng., 27, 319, 1982.
8. F. J. Cogswell et al., "Monitoring large superconducting magnets using acoustic emission technology," paper presented at the Cryogenic Engineering Conference, Cambridge, Mass., August 12-16, 1985.

Received by OSTI

NOV 04 1986

## **DISCLAIMER**

This report was prepared as an account of work sponsored by an agency of the United States Government. Neither the United States Government nor any agency thereof, nor any of their employees, makes any warranty, express or implied, or assumes any legal liability or responsibility for the accuracy, completeness, or usefulness of any information, apparatus, product, or process disclosed, or represents that its use would not infringe privately owned rights. Reference herein to any specific commercial product, process, or service by trade name, trademark, manufacturer, or otherwise does not necessarily constitute or imply its endorsement, recommendation, or favoring by the United States Government or any agency thereof. The views and opinions of authors expressed herein do not necessarily state or reflect those of the United States Government or any agency thereof.